UCRL-53697

Condensation of Ablated First-Wall Materials in the Cascade Inertial Confinement Fusion Reactor

A. J. C. Ladd

December 18, 1985

DISCLAIMER

Work performed under the auspices of the U.S. Department of Energy by Lawrence Livermore National Laboratory under Contract W-7405-Eng-48.

UCRL-53697
Distribution Category UC-21

Condensation of Ablated First-Wall Materials in the Cascade Inertial Confinement Fusion Reactor

A. J. C. Ladd

Manuscript date: December 18, 1985

LAWRENCE LIVERMORE NATIONAL LABORATORY
University of California • Livermore, California • 94550

Available from: National Technical Information Service • U.S. Department of Commerce
5285 Port Royal Road • Springfield, VA 22161 • A02 • (Microfiche A01)

Contents

Glossary

α	Degree of dissociation
β	Condensation coefficient
γ	Ratio of specific heats c_p/c_v
μ	Reduced mass
η	Packing fraction of the granular bed
ν	Bond vibration frequency
ν_n	Collision frequency of n-body collisions, $n = 1, 2, 3, \ldots$
ν_n^0	Collision frequency of n-body collisions at reference density ρ_0
ρ	Mass density
σ	Collision diameter
σ_c	Collision cross section
σ_s	Rotational symmetry number
τ	Condensation decay time
E_d	Dissociation energy
g	Electronic degeneracy
k	Boltzmann's constant
l	Mean free path
m	Molecular mass
M	Total mass
n	Number density
q	Single-molecule partition function
Q	Total partition function
r_e	Equilibrium bond distance
t_c	Condensation time
t_0	Time to beginning of condensation
T	Temperature
v	Thermal velocity of gas molecules
v_c	Condensation velocity
v_s	Shock speed
V	Chamber volume

Condensation of Ablated First-Wall Materials in the Cascade Inertial Confinement Fusion Reactor

Abstract

This report concerns problems involved in recondensing first-wall materials vaporized by x rays and pellet debris in the Cascade inertial confinement fusion reactor. It examines three proposed first-wall materials, beryllium oxide (BeO), silicon carbide (SiC), and pyrolytic graphite (C), paying particular attention to the chemical equilibrium and kinetics of the vaporized gases. The major results of this study are as follows.

Ceramic materials composed of diatomic molecules, such as BeO and SiC, exist as highly dissociated species after vaporization. The low gas density precludes significant recombination during times of interest (i.e., less than 0.1 s). The dissociated species (Be, O, Si, and C) are, except for carbon, quite volatile and are thermodynamically stable as a vapor under the high temperature and low density found in Cascade. These materials are thus unsuitable as first-wall materials.

This difficulty is avoided with pyrolytic graphite. Since the condensation coefficient of monatomic carbon vapor ($\sim$0.5) is greater than that of the polyatomic vapor ($<$0.1), recondensation is assisted by the expected high degree of dissociation.

The proposed 10-layer granular carbon bed is sufficient to condense all the carbon vapor before it penetrates to the BeO layer below. The effective condensation coefficient of the porous bed is about 50% greater than that of a smooth wall.

An estimate of the mass flux leaving the chamber results in a condensation time for a carbon first wall of about 30 to 50 ms. An experiment to investigate condensation in a Cascade-like chamber is proposed.

1. Introduction

A critical consideration in the design of an inertial confinement fusion (ICF) reactor is the condensation time of the gaseous materials vaporized by the large amounts of energy released by the fusion reactions and deposited in the form of x rays and pellet debris. Economics dictates a pulse rate of 1 to 10 Hz, and the pressure in the chamber must be reduced to less than 10^{-1} to 10^{-4} Torr (depending on the choice of driver) within the interpulse time of 0.1 to 1 s.

In this paper I consider several effects, and in particular, questions of chemical equilibrium and kinetics, that may greatly reduce the condensation rate. Rough estimates are made to identify important effects that should be included in future reactor simulations. These estimates also show that the choice of suitable first-wall materials is limited.

Although all the calculations described here apply to the Cascade reactor (Fig. 1), similar considerations are important in the design of any ICF reactor.

A complete description of the vaporization of first-wall materials by the x rays released in each fusion pulse requires a complex computer code. A simulation[1] of the HYLIFE liquid-lithium reactor included the vaporization of the lithium by the x rays, the subsequent hydrodynamics and radiation transport, and the condensation of the cooled gas. A similar description of the Cascade reactor is

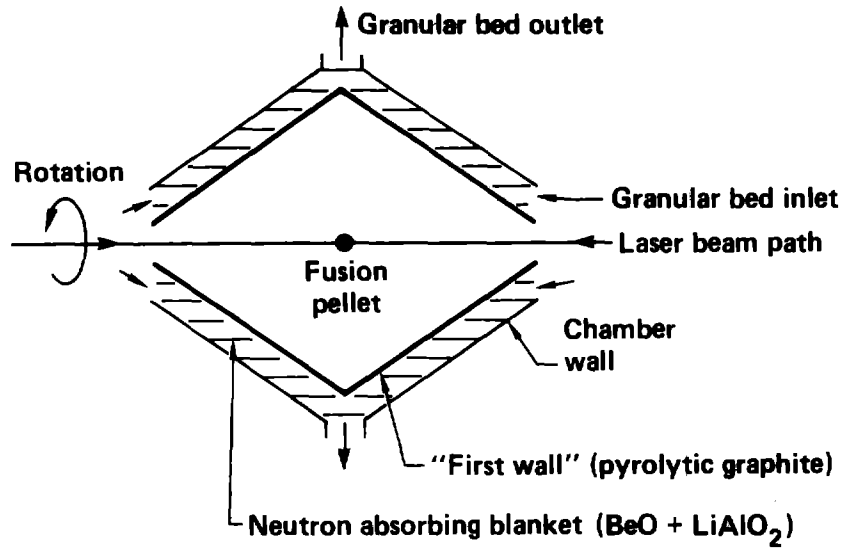

Figure 1. Sketch of the Cascade ICF reactor. The axisymmetric chamber rotates at 50 rpm. The resulting centrifugal forces keep the granular materials against the wall, and an appropriate ordering of densities keeps the various layers separate. The first-wall layer is approximately 1 cm thick; the overall blanket thickness is 1 m. The current choice of blanket materials is shown in parentheses. The blanket granules are injected at the ends of the chamber and are recovered, after several fusion pulses, from the middle of the chamber and recycled to extract heat and tritium.

more complicated because of the complex chemistry of the vaporized ceramic materials used in the first-wall layer. Several materials have been considered: beryllium oxide, (BeO), silicon carbide, (SiC), and pyrolytic graphite (C). Despite the complexity of the system, simple assumptions can be used to deduce bounds on the condensation time, and conclusions can be drawn as to the feasibility of the various materials from a condensation standpoint.

X-ray deposition profiles[2] indicate that about 1 kg of material is vaporized by the approximately 10^8 J of x-ray and pellet debris energy, and that the total amount of material vaporized is insensitive to the x-ray spectrum produced by the fusion pulse. The vaporized material expands adiabatically as it flows into the chamber. The gas is recompressed and heated as it converges on the center of the chamber. A substantial portion of the thermal energy is radiated to the first-wall layer, ablating more material.

A strong shock wave then expands outwards, losing strength as it does because of the diverging geometry. For purposes of calculation, we regard condensation as beginning when this shock wave reaches the first-wall layer, typically less than 10^{-3} s after vaporization begins. Hydrodynamic calculations on HYLIFE[1] and Cascade[3] indicate that the density and temperature are roughly uniform throughout the chamber at this time, radiation transport has essentially finished, and the degree of ionization is low, at least near the first wall. The temperature inside the chamber is between 0.5 and 1.0 eV. Substantial fluctuations in density and temperature are caused by the shock waves bouncing back and forth, but to a first approximation it can be assumed that the gas is stationary and at uniform density and temperature, and that its total mass M_0 is equal to that initially vaporized.

2. Kinetic Theory of Condensation

To estimate condensation rates, we assume that the Cascade chamber is spherical, with radius R, initial density $\rho_0 = 3M_0/4\pi R^3$, and temperature T. The number of molecules per unit volume with velocity in the range $(\mathbf{v}, \mathbf{v} + d\mathbf{v})$ is $nf(\mathbf{v};T)\,d\mathbf{v}$, where $n = \rho/m$ is the number density, m is the

molecular mass, and $f(\mathbf{v};T)$ is the single-molecule velocity distribution function. For a gas at equilibrium, f is a Maxwell-Boltzmann distribution,

$$f(\mathbf{v};T) = \left(\frac{m}{2\pi kT}\right)^{3/2} \exp\left(-mv^2/2kT\right),$$

where k is Boltzmann's constant. If we choose a coordinate system in which v_1 is perpendicular to the chamber wall and v_2 and v_3 are parallel to it, then the flux of molecules onto the wall, i.e., the number of molecules hitting unit area of the wall in unit time, is

$$\int_0^\infty dv_1 \int_{-\infty}^{\infty} dv_2 \int_{-\infty}^{\infty} dv_3\, nf(\mathbf{v})\, v_1 = n\left(\frac{kT}{2\pi m}\right)^{1/2}. \qquad (1)$$

The simplest method of describing the condensation of a gas on a solid or liquid surface is by means of the condensation coefficient $\beta(T)$, defined as the fraction of incoming molecules absorbed by the surface. We use v_c to designate the

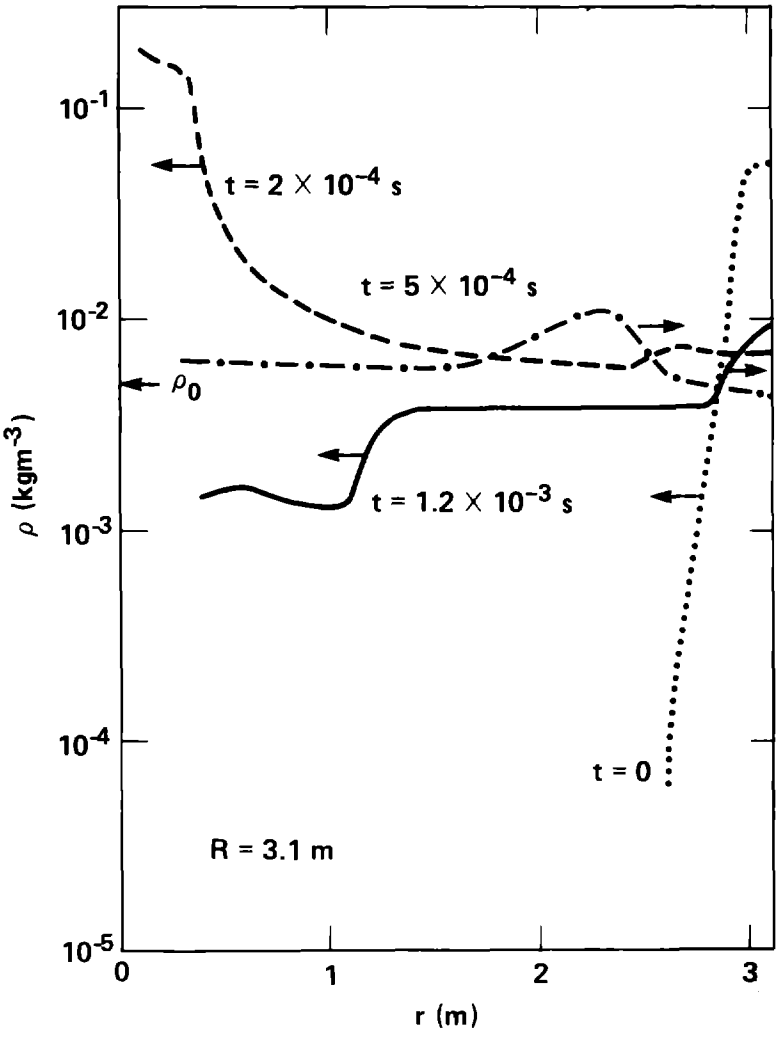

Figure 2. Typical density profiles in Cascade during blowoff and the beginning of condensation. The data are taken from a CONRAD run,[3] described in the text. The $t = 0$ curve shows the density profile just after the initial vaporization. The material is mostly confined to the outer 20 cm of the chamber. At $t = 2 \times 10^{-4}$ s, the hot gas converges on the chamber axis and reaches the maximum density obtained in the simulation. At $t = 5 \times 10^{-4}$ s, the first outgoing shock reaches the outside of the chamber. At this time most of the gas is at a uniform density, and only about 5% of the original mass has condensed. The arrow on the ρ axis indicates the uniform density ρ_0 assumed for the dissociation equilibrium and kinetics calculations, at the beginning of condensation. Later, at $t = 1.2 \times 10^{-3}$ s, shock waves bouncing back and forth cause substantial variation in density, but the uniform-density assumption is still useful. The arrows on the density profiles show the direction of shock-wave propagation at the corresponding times.

condensation velocity, i.e., the net outflow velocity at the surface, defined as

$$v_c = \beta\left(\frac{kT}{2\pi m}\right)^{1/2};$$

this velocity is to be distinguished from the fluid velocity at the wall, which is assumed to be zero. In fact v_c is a relatively small fraction (of the order of 0.3β) of the local sound speed $(\gamma kT/m)^{1/2}$, where $\gamma = c_p/c_v = 5/3$ for an ideal monatomic gas.

If we ignore hydrodynamic effects, and assume that the density remains uniform and the temperature remains constant, then the rate at which gas leaves the chamber by condensing onto the solid is given by

$$\dot{M} = -4\pi R^2 \rho v_c .$$

This leads to an exponential decay of the density with time,

$$\rho(t) = \rho(0)\, e^{-t/\tau},$$

where the decay time τ is given by

$$\tau^{-1} = \frac{3v_c}{R} = 3\beta\left(\frac{kT}{2\pi m R^2}\right)^{1/2}.$$

The adequacy of this model can be tested by comparing the predicted value of τ with results from a hydrodynamics-code run[3] in which spherical geometry was assumed and in which ionization equilibrium and radiation transport were included. The simulation modeled the blowoff of condensed, superheated BeO just after vaporization, and its recondensation onto the wall. The gas converges on the center of the chamber in about 2×10^{-4} s. Shortly afterwards it reaches approximately uniform density and temperature, although the density varies by about an order of magnitude as successive shocks bounce back and forth. The density profiles at several times are shown in Fig. 2. The decay of the average density, and the predicted decay from the kinetic theory, are shown in Fig. 3. The appropriate parameters were $m = 4 \times 10^{-26}$ kg, $R = 3.1$ m, and $\beta = 1$. The temperature at the outside of the chamber varies between 0.1 and 0.2 eV during most of the condensation process; the average temperature, 0.13 eV, was used in estimating the decay time.

The simple kinetic theory agrees with the results of the hydrodynamic calculation. This is probably because the condensation velocity v_c ($\sim$300 m s^{-1} at $T = 0.13$ eV) is considerably less than the sound speed ($\sim$1000 m s^{-1}), so that condensation is the rate-determining step. This agreement is useful in that it permits relatively simple estimates of the condensation time to be made.

To reduce the pressure to 10^{-1} to 10^{-2} Torr at a temperature of 0.15 eV requires a number density below 2×10^{21} to 2×10^{20} m^{-3}. The initial number density is about 2×10^{23} m^{-3}, so a reduction in density by a factor of 100 to 1000 is required. This gives a maximum condensation time

$$t_c = \ln(1000)\tau \simeq 6.9\tau .$$

The decay times for the materials considered here are about 4×10^{-3} s, so a reasonable lower bound to the condensation time is about 0.025 s. This is well within the required 0.1 to 1 s, so in subsequent sections I examine effects that may increase the condensation time.

3. Dissociation Equilibria and Kinetics

An important consideration in selecting a first-wall material is the chemical and ionization states of the vaporized gases, since the subsequent recondensation processes can be greatly altered by changes in chemical and, to a lesser extent, ionization states.

Vaporization of first-wall materials such as BeO and SiC will give rise to partially dissociated gases. With the possible exception of carbon vapor, these dissociated gases (Be + 1/2 O_2 and Si + C) will not recondense onto the walls under the conditions found in Cascade. This can be deduced from thermodynamic considerations alone. The wall temperature in Cascade is about 1600 to 2200 K; the corresponding vapor pressures of beryllium and silicon are about 10 to 100 Torr, and O_2 is, of course, above its critical point. All these vapor pressures are well above the maximum laser-firing pressure of 0.1 Torr, and it would therefore be necessary to pump gas out. However, the maximum pumping capacity of the Cascade system is about 10^5 L s^{-1}; at a final pressure of 0.1 Torr and a temperature of 1600 K, this corresponds to the production of about 10^{-2} gram-moles (i.e., less than 1 g) of dissociated gas per pulse, for a repetition rate of 10 Hz. In this section

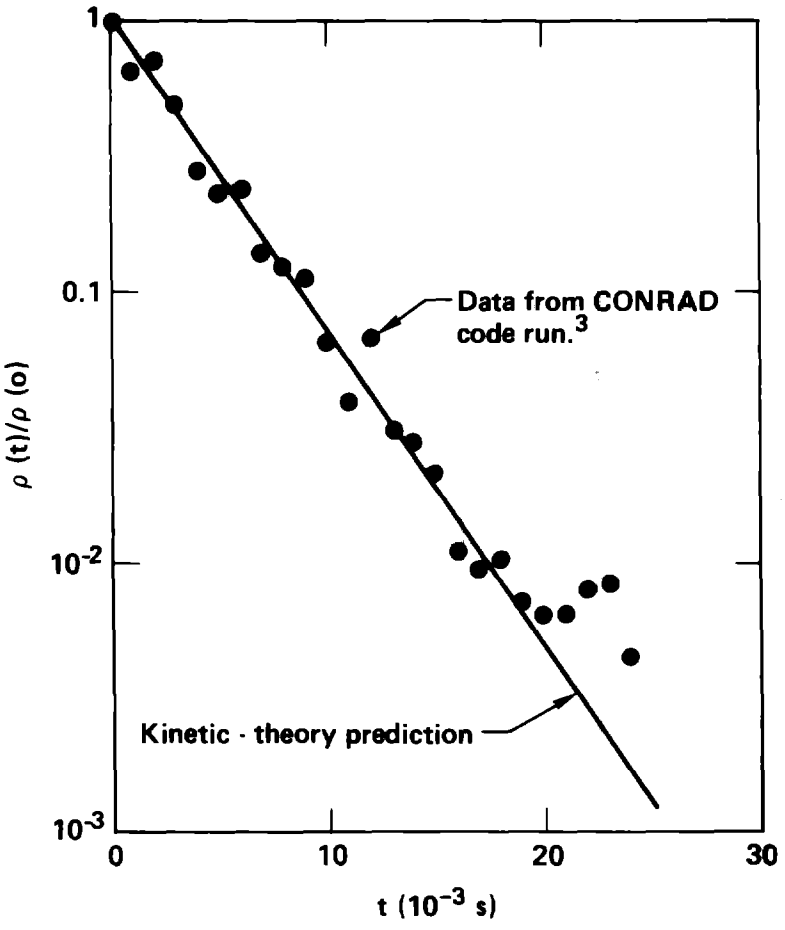

Figure 3. Average density in the Cascade chamber at various times during condensation (data points), as given by the CONRAD simulation.[3] After about 2×10^{-3} s (third data point), the temperature in the zone next to the wall fluctuates between 0.1 and 0.2 eV, as the shock waves bounce back and forth. The average of these temperatures, $T = 0.13$ eV, is used in the kinetic-theory calculation described in the text. The resulting decay time $\tau = 3.7 \times 10^{-3}$ s is the slope of the solid line.

we examine the dissociation equilibria and kinetics of these gases, to estimate the quantity of incondensible dissociated gas produced by each pulse.

Shortly after the deposition of x-ray and pellet debris energy, the gas is at a very high density and temperature; the density is close to that of the solid, and the internal energy, before dissociation and ionization, is tens of eV per molecule. If we consider the dissociation equilibrium

$$(1 - \alpha)\mathrm{AB} \leftrightarrow \alpha\mathrm{A} + \alpha\mathrm{B},$$

which could represent either chemical dissociation or ionization, then the degree of dissociation is inhibited by the high density of the gas just after vaporization. The expression for α is of the form

$$\alpha \propto \rho^{-n}\exp(-D_0/kT),$$

where D_0 is the dissociation energy and n is not necessarily an integer. As the gas expands into the chamber, the reduction in density by several orders of magnitude far outweighs the effect of the changing temperature, which is still of the order of the dissociation energy, so that dissociation increases as the gas expands. Dissociation probably reaches a maximum around the time that condensation begins. After this the cooling in the chamber may dominate the continued reduction in density through condensation, resulting in reduced dissociation.

The temperature in the chamber during condensation is largely fixed by radiation transport. Initially, the specific energy per molecule is about

20 to 40 eV, so that the dissociation energies, which are about 5 eV, are only a small fraction of the total energy available. The remaining energy goes into ionization, thermal energy (temperature), and kinetic energy. A substantial fraction of the total energy is lost by radiation transport, as the gas converges on the center of the chamber. Since the radiation transport mechanism has a sharp cutoff around 0.5 eV,[1] this will essentially fix the temperature of the stagnant gas at the beginning of condensation between 0.5 and 1.0 eV. In later sections, the equilibrium degree of dissociation is estimated for BeO and SiC under conditions approximating those found initially and at the beginning and end of condensation. The kinetics of the dissociation and recombination processes are then considered to arrive at a reasonable estimate of the chemical state of BeO and SiC during condensation.

A. Dissociation Equilibria of BeO and SiC

We consider the equilibrium

$$AB \leftrightarrow A + B,$$

where B represents either an atom or a molecule (i.e., 1/2 B_2). The partition function for the mixture is[4]

$$Q = \frac{(q_{AB})^{N_{AB}}(q_A)^{N_A}(q_B)^{N_B}}{(N_{AB})!\,(N_A)!\,(N_B)!},$$

where for an ideal gas the single-molecule partition functions q are functions of V and T only. Introducing the degree of dissociation α, we have

$$N_{AB} = N_0(1 - \alpha),$$

$$N_A = N_0\alpha,$$

$$N_B = jN_0\alpha,$$

where $j = 1/2$ if B is molecular (i.e., B = 1/2 B_2) and $j = 1$ otherwise. Since the total volume is fixed, we can calculate the degree of dissociation as a function of temperature and mass density (or, equivalently, of N_0) by minimizing the Helmholtz free energy $F = -kT \ln Q$ with respect to α: we find

$$\frac{\alpha(j\alpha)^j}{1 - \alpha} = \frac{q_A q_B^j}{q_{AB} N_0^j}.$$

The single-molecule partition functions are products of electronic and translational partition functions, and (in the case of diatomic molecules) of rotational and vibrations ones as well: that is,

$$q = q_{elec} q_{trans} q_{rot} q_{vib}.$$

If the molecules are in their electronic ground states, with energy E and degeneracy g, then[4]

$$q_{elec} = g \exp\left[-\left(E + \frac{1}{2}h\nu\right)/kT\right],$$

$$q_{trans} = \left(\frac{2\pi mkT}{h^2}\right)^{3/2} V,$$

$$q_{rot} = \frac{8\pi^2 IkT}{\sigma_s h^2},$$

$$q_{vib} = \frac{kT}{h\nu},$$

where I is the moment of inertia, σ_s is the rotational symmetry number (2 for homonuclear diatomics and 1 for heteronuclear diatomics), and ν is the vibrational frequency. For a diatomic molecule $I = \mu r_e^2$, where $\mu = m_1 m_2/(m_1 + m_2)$ is the reduced mass and r_e is the equilibrium separation. The contribution of the zero-point motion has been included in the electronic partition function because this contribution is incorporated in the usual definition of the spectroscopic dissociation energy,

$$D_0 = E_A + E_B - E_{AB} - \frac{1}{2}h\nu.$$

Thus

$$\frac{\alpha(j\alpha)^j}{1 - \alpha} = \frac{g_A g_B^j}{g_{AB} N_0^j} \exp(-D_0/kT) \frac{q'_A q'^j_B}{q'_{AB}},$$

where the partition function q' contain only translational, rotational, and vibrational contributions.

For future reference we calculate various partition functions at a reference state in which T_0 = 1 eV:

$$(q_0)_{\text{trans}} = \left(\frac{2\pi m_p k T_0}{h^2}\right)^{3/2} V$$

$$= 2.4 \times 10^{32} V \,(V \text{ in m}^3),$$

$$(q_0)_{\text{rot}} = \frac{8\pi^2 m_p r_0^2 k T_0}{h^2} = 4.8 \times 10^2,$$

$$(q_0)_{\text{vib}} = \frac{k T_0}{h \nu_0} = 8.1,$$

where m_p is the proton mass, $r_0 = 10^{-10}$ m, $I_0 = m_p r_0^2$, and $\nu_0 = 1000\ \text{cm}^{-1} = 3 \times 10^{13}\ \text{s}^{-1}$. The partition functions for the electronic ground states of BeO, SiC, and O_2 have been calculated and are given in Table 1.

The equilibrium degrees of dissociation of BeO,

$$\frac{\alpha^{3/2}}{1-\alpha} = 8.7 \times 10^2 \left(\frac{T_0}{T}\right)^{1/4} \left(\frac{\rho_0}{\rho}\right)^{1/2} \exp\left(-2.0 T_0/T\right)$$

and of SiC,

$$\frac{\alpha^2}{1-\alpha} = 2.2 \times 10^6 \left(\frac{T_0}{T}\right)^{1/2} \left(\frac{\rho_0}{\rho}\right) \exp\left(-4.6 T_0/T\right). \quad (2)$$

Table 1. The partition functions of BeO, SiC, and O_2 are shown, using the spectroscopic data of Ref. 5, which is an expansion and update of Ref. 6. In the row labeled g, the electronic degeneracy of the molecular state is shown followed by the degeneracy of the constituent atoms. All partition functions are evaluated at a reference temperature of 1 eV.

	BeO	SiC	O_2
D_0 (eV)	4.6	4.6	5.1
r_e (Å)	1.3	1.8	1.2
ν (cm^{-1})	1500	1000	1600
g	1, 1, 3	3, 3, 3	3, 3, 3
q_{trans}/V (m^{-3})	3.0×10^{34}	6.1×10^{34}	1.5×10^{34}
q_{rot}	4.7×10^3	1.3×10^4	2.8×10^3
q_{vib}	5.4	8.1	5.1
q'/V (m^{-3})	7.6×10^{38}	6.4×10^{39}	2.1×10^{38}

are shown in Table 2 at the density of the material at vaporization ($\rho = 6 \times 10^5 \rho_0 = 3 \times 10^3\ \text{kg m}^{-3}$), the beginning of condensation ($\rho = \rho_0 = 5 \times 10^{-3}\ \text{kg m}^{-3}$), and at the end of condensation ($\rho = 10^{-3} \rho_0 = 5 \times 10^{-6}\ \text{kg m}^{-3}$). Representative temperatures are shown at each density. The formulas for the degrees of dissociation are derived from the partition functions in Table 1.

The results in Table 2 show that material is vaporized with a significant amount of dissociation. Thermodynamically, dissociation increases during blowoff, because of the rapid decrease in density, but this is gradually compensated for by the cooling in the chamber, so that the degree of dissociation eventually becomes small. This is shown qualitatively in Fig. 4, curve A. However, because of the generally low gas density, both dissociation and recombination may be kinetically inhibited, as shown in curves B, C, and D. In Secs. 3(B), (C), and (D) we show that dissociation is in fact uninhibited, while recombination is basically prevented, so that curve B illustrates the situation to be expected in Cascade, with the degree of dissociation remaining high.

Table 2. Dissociation equilibria of BeO and SiC. The degrees of dissociation α of BeO and SiC are calculated from equilibrium statistical mechanics, using an ideal-gas equation of state. The required partition functions are taken from Table 1. Three densities have been used, corresponding roughly to that of newly vaporized material ($\rho = 3 \times 10^3\ \text{kg m}^{-3}$); that of the same material distributed uniformly in the chamber, which is an idealization of the situation when blowoff ends and condensation begins ($\rho = 5 \times 10^{-3}\ \text{kg m}^{-3}$); and that at the end of condensation ($\rho = 5 \times 10^{-6}\ \text{kg m}^{-3}$). The two temperatures shown for each density are estimates of the lowest and highest possible temperatures at these states. Only in the final state is the dissociation state really sensitive to temperature, varying from 0 to 1 over a plausible range of temperature.

ρ (kg m^{-3})	T (eV)	α_{BeO}	α_{SiC}
3×10^3	1.0	0.2	0.2
3×10^3	4.0	0.4	0.5
5×10^{-3}	0.5	1.0	1.0
5×10^{-3}	1.0	1.0	1.0
5×10^{-6}	0.1	0.0	0.0
5×10^{-6}	0.5	1.0	1.0

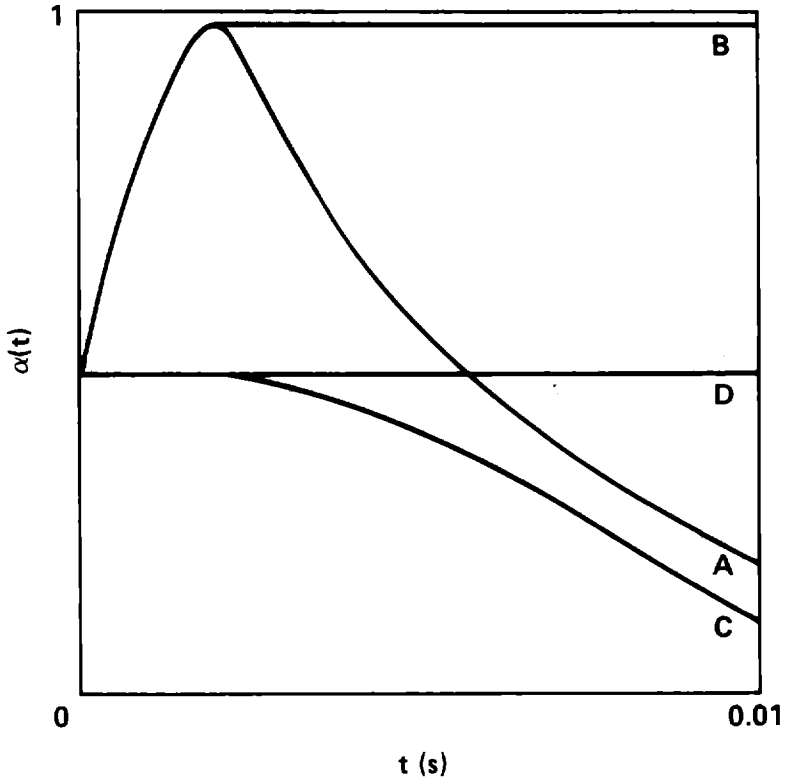

Figure 4. Degree of dissociation of diatomic molecules in Cascade. This sketch indicates in a qualitative way the possible time history of the degree of dissociation. In curve A the kinetics of dissociation and recombination are considered to be instantaneous, so that the equilibrium curve is followed. Curve B represents the situation actually found in Cascade: rapid dissociation kinetics and slow recombination kinetics. Curve C shows the reverse situation, slow dissociation and rapid recombination. In curve D, both dissociation and recombination are slow.

B. Chemical Reaction Rates and Collision Rates

We are interested in the kinetics of the dissociation reaction

$$AB + X \rightarrow A + B + X$$

and the subsequent recombination

$$A + B + X \rightarrow AB + X,$$

where X can be any species AB, A, or B. These reactions are discussed, for example, in Ch. 9 of Ref. 7, and only a simplified discussion suitable for rough estimates is given here. We ignore the quantitative distinctions between B and 1/2 B_2, and assume that dissociation products are all atomic.

The kinetics of the dissociation reaction are described by the equation

$$\frac{dn_{AB}}{dt} = -k_d \exp\left(-E_d/kT\right) n_{AB} \nu_2 ,$$

where ν_2 is the rate at which a particular AB molecule collides with any species X and where we assume that collisions with any species are equally effective in causing dissociation. The collision rate ν_2 is proportional to the total number density, $n_{AB} + n_A + n_B$. The exponential factor represents the probability that the colliding pair has enough energy to overcome the activation barrier to dissociation. We assume that this is equal to the dissociation energy. The remaining factor k_d reflects the fact that not all collisions of appropriate energy result in dissociation. For convenience we refer all calculations to a standard

state in which the material, assumed to be undissociated, is uniformly distributed throughout the chamber, with a mass density $\rho_0 = 5 \times 10^{-3}$ kg m^{-3}. Thus an equation for the kinetics of dissociation is

$$\dot{\alpha} = k_d \exp(-E_d/kT)(1 - \alpha^2)(\rho/\rho_0)\nu_2^0,$$

where α is the degree of dissociation and ν_2^0 is the two-body collision rate at the reference density ρ_0.

Similarly for the recombination reaction, which is assumed not to have an activation barrier,

$$\dot{\alpha} = -k_r\alpha^2(1 + \alpha)(\rho/\rho_0)^2\nu_3^0,$$

where ν_3^0 is the rate of collision at density ρ_0 of a "quasi molecule" (that is, two atoms in close contact) with another atom. At equilibrium, the dissociation and recombination rates must be equal, and thus we have for the equilibrium degree of dissociation

$$\frac{\alpha^2}{1 - \alpha} = \frac{k_d\nu_2^0}{k_r\nu_3^0}(\rho_0/\rho)\exp(-E_d/kT),$$

an expression similar to Eq. (2) found earlier for SiC from equilibrium considerations alone.

The two-body collision rate can be estimated from the volume ΔV swept out in time Δt by a molecule traveling at a speed v equal to the thermal velocity $(kT/m)^{1/2}$, i.e.,

$$\Delta V = \pi\sigma^2 v\,\Delta t,$$

where σ is the collision diameter.

The collision rate ν_2^0 is then approximately $(N\,\Delta V)/(V\,\Delta t)$, i.e.,

$$\nu_2^0 = vn_0\sigma_c,$$

where $n_0 = \rho_0/m$ is the reference number density and $\sigma_c = \pi\sigma^2$ is the collision cross section.

Pairs of atoms come together for a short time $\sim\sigma/v$ every mean collision time $(\nu_2^0)^{-1}$; thus the fraction of atom pairs in close enough contact for chemical reaction is $\sigma\nu_2^0/v = \pi n_0\sigma^3$. The reference three-body collision frequency is therefore

$$\nu_3^0 = \pi n_0\sigma^3\nu_2^0.$$

The thermal velocity at $T_0 = 0.5$ eV is about 10^3 m s^{-1}. A typical collision cross section for a chemical reaction is about 10^{-19} m^2, and the number density is about 10^{23} m^{-3}. Thus

$$\nu_2^0 \simeq 10^7 \text{ to } 10^8 \text{ s}^{-1},$$

$$\nu_3^0 \simeq 10 \text{ to } 100 \text{ s}^{-1}.$$

C. Dissociation Kinetics Before Condensation

During blowoff, which occurs during the first millisecond, the rapidly decreasing density drives the chemical equilibrium towards increased dissociation. In this section we examine the kinetics of this process. We assume that during blowoff the gas front advances at a constant speed $v_s = R/t_0$, where t_0 is the time at which the gas first converges on the center of the chamber. Then

$$\dot{n} = \dot{\rho}/m = -\frac{9Mv_s(R - v_st)^2}{4\pi m\left[R^3 - (R - v_st)^3\right]^2}.$$

The kinetics of the collision-induced dissociation reaction, AB + X → A + B + X, where X = A, B, or AB, is given by[7] [see Sec. 3(B)]

$$\dot{n}_A = \dot{n}_B = -\dot{n}_{AB} = k_d n_{AB}(n_A + n_B + n_{AB}) \times \exp(-E_d/kT)\,\nu_2^0/n_0,$$

where we have assumed that the activation energy for dissociation is the same as the dissociation energy E_d. The two-body collision frequency ν_2^0, evaluated for undissociated gas at the reference state $\rho_0 = 5 \times 10^{-3}$ kg m^{-3}, $T = 0.5$ eV, was calculated in Sec. 3(B). In terms of the reduced variables $x \equiv \rho/\rho_0$, $\alpha \equiv n_A/n$, we have

$$\dot{x} = (\dot{\rho}/\rho_0) = -\frac{3v_sR^3(R - v_st)^2}{\left[R^3 - (R - v_st)^3\right]^2} = \frac{-3(1 - t/t_0)^2}{t_0\left[1 - (1 - t/t_0)^3\right]^2},$$

$$\dot{\alpha} = k_d\nu_2^0\exp(-E_d/kT)(1 - \alpha^2)x.$$

The mass density $\rho(t)$ has a maximum value of about 3×10^3 kg m^{-3}, about 10^6 times the uniform reference density of about 5×10^{-3} kg m^{-3}. The divergence of $\rho(t)$ at $t = 0$ is most easily

taken care of by setting the starting time $t_s = 10^{-6}t_0$: then our equation for α is

$$\frac{1+\alpha}{1-\alpha} = \frac{1+\alpha_s}{1-\alpha_s} e^{\Omega(t)},$$

$$\Omega(t) = k_d \nu_2^0 \exp(-E_d/kT) \int_{t_s}^{t} \frac{dt'}{\left[1-(1-t'/t_0)^3\right]}$$

$$\simeq \frac{1}{3} k_d \nu_2^0 t_0 \exp(-E_d/kT) \ln(t/t_s),$$

where α_s is the degree of dissociation of the newly vaporized material. Thus by the time t_0, when the gas has first converged on the center of the chamber, the degree of dissociation α_0 is given by

$$\frac{1+\alpha_0}{1-\alpha_0} = \frac{1+\alpha_s}{1-\alpha_s} e^{\Omega_0},$$

where

$$\Omega_0 = 5 k_r \nu_2^0 t_0 \exp(-E_d/kT).$$

The gas converges on the center of the chamber in about 2×10^{-4} s, and using an estimate of ν_2^0 of $5 \times 10^7\ s^{-1}$, we find $\Omega_0 \simeq 10^5 \exp(-E_d/kT)$. Thus dissociation is kinetically uninhibited if $E_d < 10kT$. The temperature in the chamber is generally several eV during blowoff and is always at least 0.5 eV. Thus dissociation is in general uninhibited; for example, both BeO and SiC have dissociation energies of 4.6 eV. In these cases the value of Ω_0 (for $\nu_2^0 = 5 \times 10^7\ s^{-1}$, $T = 0.5$ eV) is about 10, so that (at the beginning of condensation) dissociation is essentially complete (i.e., $\alpha_0 = 1$), regardless of the starting dissociation α_s.

D. Recombination Rates During Condensation

We consider the beginning of condensation as a starting point, and assume that the gas is uniform and stationary, with density $\rho_0 = M_0/V$, where M_0 is the mass of material vaporized and V is the chamber volume. The two- and three-body collision frequencies (that is, the rates at which an atom or molecule undergoes collisions with one or two other particles) can be calculated from kinetic theory,[7] as shown in Sec. 3(B).

The recombination reaction involves three-body collisions, A + B + X, where X = A, B, or AB; the kinetics of such collisions can be described by the rate equations

$$\dot{n}_A = \dot{n}_B = -k_r n_A n_B (n_A + n_B + n_{AB}) \nu_3^0 / n_0^2,$$

$$\dot{n}_{AB} = -\frac{n_{AB}}{\tau} + k_r n_A n_B (n_A + n_B + n_{AB}) \nu_3^0 / n_0^2,$$

where $n_0 = \rho_0/m$ is the number density of AB molecules in the absence of dissociation and before recondensation, and k_r is a steric factor that accounts for the fact that not all collisions result in recombination. The first term in the second equation describes the condensation of AB molecules; we assume that A and B are volatile and do not condense. Combining these equations, we find that

$$\frac{\dot{M}}{M} = \frac{\dot{\rho}}{\rho} = -\frac{(1-\alpha)}{\tau}, \tag{3}$$

$$\dot{\alpha} - \alpha \frac{(1-\alpha)}{\tau} = -k_r \nu_3^0 \alpha^2 (1+\alpha) (\rho/\rho_0)^2. \tag{4}$$

Equation (3) describes the rate of mass condensation, which is proportional to the number of AB molecules; when $\alpha = 1$, there are no AB molecules and condensation stops. The degree of dissociation is driven upwards by the condensation, which in the absence of recombination increases the proportion of dissociated species. If $k_r \nu_3^0 \tau \ll 1$, then recombination is essentially frozen during condensation and the condensation is incomplete:

$$M(t) = M_0 \left[\alpha_0 + (1-\alpha_0) e^{-t/\tau}\right],$$

$$\frac{\alpha}{1-\alpha} = \frac{\alpha_0}{1-\alpha_0} e^{t/\tau}.$$

The degree of dissociation rises from its initial value α_0 to unity, whereupon condensation stops. The uncondensed mass remaining in the chamber is αM_0. Since $\nu_3^0 \tau$ is estimated to be of the order of 10^{-2} to 10^{-1}, this case is probably the appropriate one, especially if k_r is much less than unity. If recombination is frozen at the beginning of condensation, the degree of dissociation must be very small, i.e., less than 10^{-4}, or else unacceptably large amounts of incondensible dissociated gas will be produced.

Another case that might be important is the one in which recombination and condensation initially proceed at about the same rate; i.e., when

$k_r \nu_3^0 \tau \simeq 1$. If the degree of dissociation is initially small, i.e., if $\alpha_0 \ll 1$, then this case of course reduces to the one described above. We consider specifically the case in which $k_r \nu_3^0 \tau = 1$. The cubic term in α in Eq. (4) is qualitatively unimportant, since α is always less than unity. It reflects only small changes in the number of third bodies X in the A + B + X collision and will be ignored. Thus the equations become

$$\dot{x} = -\left(\frac{1 - \alpha}{\tau}\right)x,$$

$$\dot{\alpha} = \frac{\alpha(1 - \alpha) - \alpha^2 x^2}{\tau}.$$

The equation for α can be rewritten more instructively as

$$\frac{d}{dt}\ln\left(\frac{\alpha}{1 - \alpha}\right) = \frac{1 - \alpha^2 x^2}{\tau}.$$

When $\alpha^2 x^2 \ll 1$, recombination is unimportant, and the degree of dissociation rises as the molecular material condenses, so that the mass of dissociated species is constant. Therefore, even if $k_r \nu_3^0 \tau$ is of order unity, recombination is important only if the initial dissociation is high. We consider the case for which $\alpha_0 = 1$, so that $\dot{x} = 0$ initially. Ignoring condensation, we have

$$\frac{d}{dt}\ln\left(\frac{\alpha}{1 - \alpha}\right) = \frac{1 - \alpha^2}{\tau},$$

or

$$\frac{\alpha}{(1 - 2\alpha)} = \frac{\alpha_0}{(1 - 2\alpha_0)}e^{t/\tau},$$

that is,

$$\frac{\alpha}{2\alpha - 1} = e^{t/\tau}$$

for $\alpha_0 = 1$, so that in a time of the order τ, α has decreased to close to a fixed value of 0.5. Condensation begins as α drops, so that after a time τ, the recombination rate $\dot{\alpha}$ is close to the maximum of $0.5\tau^{-1}$, as against a rate of τ^{-1}, which is obtained when there is no dissociation. At the beginning of condensation, α is roughly constant, but as x decreases recombination slows and α begins to increase again. After about 2 to 3τ, x has dropped to about 0.3, so that $x^2 \simeq 0.1$. Recombination becomes negligible, and the amount of dissociated material becomes fixed. Thus the amount of incondensible material is about $\alpha x M_0$, i.e., about 15% of the initially vaporized material, or 150 g.

Thus a small initial degree of dissociation is essentially frozen, even if $k_r \nu_3^0 \tau \simeq 1$. With a high degree of dissociation, some recombination could possibly take place, but about 100 g of dissociated material would remain after each pulse. Only if $k_r \nu_3^0 \tau \gg 1$ could enough recombination occur to satisfy the driver-firing conditions, and this cannot occur under the conditions found in Cascade during condensation because the density is much too low.

E. Dissociation of BeO and SiC in Cascade

We have shown that, under the conditions found in Cascade, dissociation during blowoff is kinetically uninhibited and the gas reaches the equilibrium prediction of complete dissociation by the time condensation begins. Recombination of the gas as the chamber cools is kinetically inhibited, so that the degree of dissociation remains high, as illustrated in Fig. 4, curve B. Since the dissociated species (Be and O_2, or Si and C) are, with the exception of carbon, in the vapor state at the low pressures found during most of the condensation process, BeO and SiC are unsuitable as first-wall materials. Even if the dissociated materials are nonvolatile, the condensation of, say, carbon vapor on a noncommensurate surface such as SiC is not likely to be rapid. Thus diatomic or polyatomic materials would, in general, not be suitable as first-wall materials in Cascade. In subsequent sections, we examine the recondensation of carbon, which seems a more promising first-wall material.

4. Carbon Condensation

A. Dissociation Equilibrium of Carbon Vapor

The dissociation equilibrium of carbon is quite complex; at pressures above 1 atm, the gas exists as a mixture of carbon chains C_n, where n varies from 1 to about 7 (Ref. 8). The composition of carbon vapor over solid or liquid carbon is described in Ref. 8. At low enough pressure the monatomic form C_1 is dominant; the next most important species is C_3, rather than C_2, because of the anomalous stability of C_3. For simplicity we examine the $C_1 \leftrightarrow C_3$ equilibrium, i.e.,

$$(1 - \alpha)C_3 \leftrightarrow 3\alpha C .$$

Using the methods described in the previous section, we find an expression for the degree of dissociation of the form

$$\frac{\alpha^3}{1 - \alpha} \propto \left(\frac{V}{N_0}\right)^2 \frac{1}{T^2} \exp\left(-D_0/kT\right).$$

Assuming an ideal-gas equation of state,

$$pV = NkT = N_0(1 + 2\alpha)kT = p_0V(1 + 2\alpha),$$

we find

$$b \equiv \frac{\alpha^3}{(1 - \alpha)(1 + 2\alpha)^2} = Ap^{-2} \exp\left(-D_0/kT\right),$$

where the value of the constant A depends on the partition functions of C_1 and C_3. We have calculated α from the relative fractions of C_1 and C_3 from the data of Leider, Krikorian, and Young,[8] as a function of temperature along the saturated vapor curve. In Fig. 5, we plot

$$\ln b = \ln \frac{\alpha^3}{(1 - \alpha)(1 + 2\alpha)^2} p^2$$

against $1/T$. The data[8] fall on a straight line corresponding to a dissociation energy of 13.9 eV, in reasonable agreement with the experimental value[8] of 13.2 eV, verifying our approximate expression for α. The constant A is about 6×10^{12} if p is in atmospheres. In Table 3 we give the degree of dissociation for carbon, based on the formula above, for the same states shown for BeO and SiC in Table 2.

The dissociation equilibrium of carbon follows trends similar to those described for BeO and SiC. The recombination of C_1 to C_3, going via C_2 molecules, is much more complex than the recombination of BeO, so that $k_r\nu_3^0\tau \ll 1$. Thus the dissociation state at the beginning of condensation is likely to be completely frozen, with no recombination taking place. Dissociation of the triatomic vapor proceeds in two steps,

$$C_3 \rightarrow C_2 + C ,$$

$$C_2 \rightarrow 2C ,$$

with a dissociation energy of about 6.5 eV for each step, so that dissociation is not likely to be kinetically inhibited, if the chamber temperature is greater than about 0.7 eV.

B. Ionization Equilibrium and Kinetics

Since a highly ionized gas may hinder condensation, we must consider the ionization equilibrium and the rate of ion-electron recombination. The collision diameter σ of a Coulomb system can be estimated by equating the potential energy e^2/r of the colliding pair with the thermal energy kT, so that σ is given by

$$\sigma \simeq e^2/kT ;$$

Table 3. Dissociation equilibria (indicated by α) of carbon. The degrees of dissociation of carbon at the same states considered in Table 2 are shown. The degrees of dissociation are calculated from the data of Ref. 8 by using the appropriate pressure correction described in the text. The pressure calculated here does not include dissociation, so the appropriate expression for b is simply $b = \alpha^3/(1 - \alpha)$.

ρ (kg m^{-3})	T (eV)	p_0 (atm)	α
3×10^3	1.0	2.4×10^5	0.0
3×10^3	4.0	9.5×10^5	0.5
5×10^{-3}	0.5	0.2	1.0
5×10^{-3}	1.0	0.4	1.0
5×10^{-6}	0.1	4.0×10^{-5}	0.0
5×10^{-6}	0.5	2.0×10^{-4}	1.0

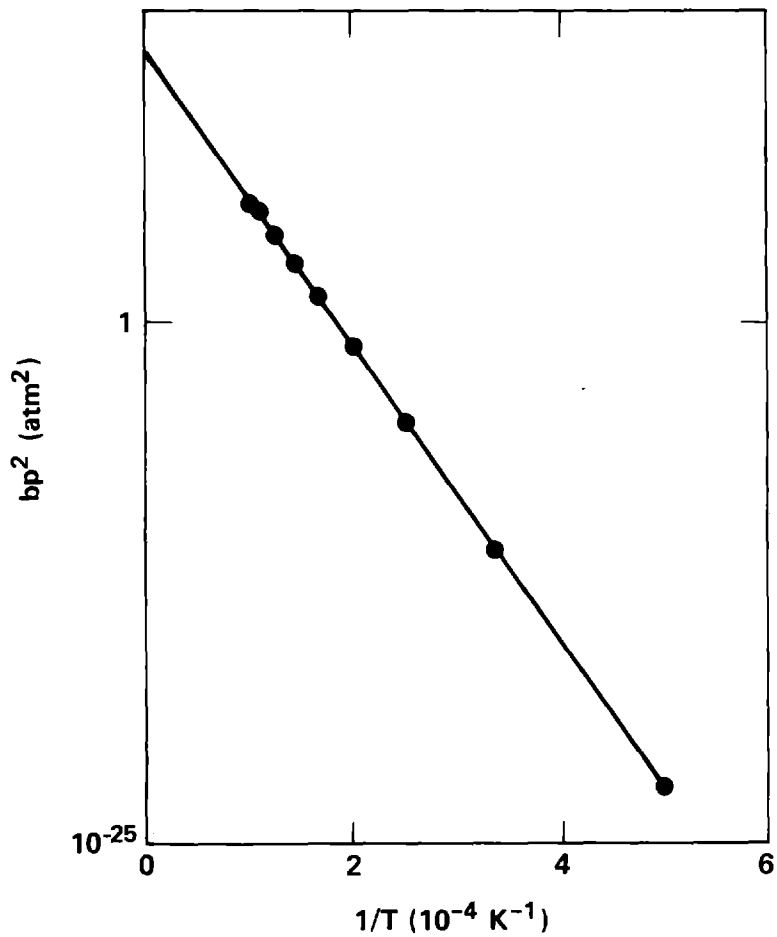

Figure 5. Theoretical and experimental degrees of dissociation of carbon. Theoretical considerations described in the text indicate that the degree of dissociation α in the $C_3 \leftrightarrow 3\ C_1$ equilibrium, at the saturated vapor pressure, obeys $bp^2 = \exp(-D_0/kT)$, where $D_0 = 13.3$ eV is the dissociation energy of C_3; the function b is defined in the text. The filled circles are the data of Ref. 8. The slope of the straight-line fit corresponds to a dissociation energy of 13.9 eV, in reasonable agreement with D_0. Thus we expect that the simple $1/p^2$ pressure correction described in the text will yield a good description of the dissociation of carbon in Cascade.

at a temperature of 0.5 eV, σ is approximately 30 Å, or about 10 times the collision diameter of chemically reacting species. Since the three-body collision frequency is proportional to σ^5, ion-electron recombination will be at least 10^5 times faster than chemical recombination. Ion-electron recombination occurs predominantly through ion-electron-electron collisions, and the appropriate three-body collision frequency is

$$\pi^2\left(\frac{e^2}{kT}\right)^5\left(\frac{kT}{m_e}\right)^{1/2}\alpha^2 n^2 \simeq -\dot{\alpha},$$

or

$$\dot{\alpha} = -A\frac{n^2}{T^{9/2}}\alpha^2.$$

This is a well-known form for the ion recombination rate equation.[9] The constant A can be calculated from quantum mechanics,[9] with the result that $A \simeq 10^{-20}\ \mathrm{s}^{-1}$ if n is in m^{-3} and T is in kelvins. Thus we find for carbon, at the beginning of condensation (with $\rho = 5 \times 10^{-3}\ \mathrm{kg}^{-3}$ and $T = 0.5$ eV),

$$\dot{\alpha} = -\nu_3\alpha^2,$$

$$\nu_3 = \frac{An^2}{T^{9/2}} \simeq 10^{10}\ \mathrm{s}^{-1}.$$

It is noteworthy that ν_3 increases rapidly as the gas cools because of the increasing collision cross section. Thus we can assume that the gas is always in ionization equilibrium.

In considering ionization equilibria, we assume that $q'_A = q'_{AB}$, i.e., that the ion and neutral-molecule partition functions are the same. Then, since the electron-gas ground state is doubly degenerate, the degree of ionization is given by

$$\frac{\alpha^2}{1-\alpha} = \frac{2}{N_0} \exp(-\mathrm{IP}/kT)\, q^{e}_{trans},$$

where IP is the ionization potential and q^{e}_{trans} is the translational partition function of an electron. For monatomic carbon vapor at the beginning of condensation ($\rho = \rho_0 = 5 \times 10^{-3}$ kg m^{-3}),

$$\frac{\alpha^2}{1-\alpha} = 2.4 \times 10^4\, T^{3/2}\, e^{-11.2/T},$$

where T is in eV, so that $\alpha \simeq 10^{-3}$ at $T = 0.5$ eV. This means that we can neglect the effects of ionization during condensation and assume that the gas is neutral.

C. Condensation Coefficients and Incondensible Gases

The condensation coefficient β, defined as the probability that a gas molecule will stick to a solid surface as a result of collision with it, gives a simplified, macroscopic description of the complex processes involved in collisions between gas molecules and solid surfaces. Theoretical considerations of the transfer of energy away from the surface by phonons exited by the impact of a gas molecule lead one to expect a condensation coefficient of unity, for a cold solid surface, unless the energy of the incident molecule is greater than about twice the latent heat of sublimation,[10] i.e., 10 to 15 eV per molecule. This has been verified experimentally for several metallic vapors condensing on their own solid phase.[11]

Carbon is an exception, however. The reflection coefficients ($1 - \beta$) of C_1 and C_3 vapor have been measured directly by Chupka et al,[11] and the closely related evaporation coefficients have been measured in a Knudsen cell.[12] In Ref. 11, the condensation coefficients β_1 and β_3 of C_1 and C_3 vapor were found to be

$$\beta_1 = 0.4 \pm 0.2,\ \beta_3 = 0.1 \pm 0.2 \text{ for } T = 2300\ \mathrm{K},$$

$$\beta_1 = 0.70 \pm 0.15,\ \beta_3 = -0.1 \pm 0.2 \text{ for } T = 800\ \mathrm{K},$$

where T is the solid-surface temperature. When the gas and solid are in thermal and mechanical equilibrium, as in a Knudsen cell, the evaporation and condensation coefficients are the same[13]; at $T = 2450$ K, these coefficients are 0.37, 0.34, and 0.08 for C_1, C_2, and C_3, respectively,[12] which is consistent with the measurements of β at 2300 K. The condensation coefficient for C_1 at 1600 K is likely to be about 0.5, and that of C_3 is essentially zero, so a high degree of dissociation is necessary for effective recondensation of carbon at this temperature. Our calculations show that this is the case.

The rate of condensation of a gas onto a condensed phase can be greatly reduced by the presence of incondensible gases.[14] The reduction depends on the relative density of incondensible and condensible gases and on the relative molecular masses; high densities of high-mass incondensibles cause the greatest reductions in condensation rate.[15] Since the incondensible gases, mainly He, DT, and T_2, must be pumped out, the permissible production rate of incondensible gas is limited by the pumping capabilities of the Cascade system to less than 0.01 gram-moles per pulse.[16] The condensible-gas density is limited only by the laser firing pressure of 10^{-1} to 10^{-2} Torr, a pressure that corresponds to at least 0.1 gram-moles of uncondensed material. Thus the incondensible-gas density can never be more than 10% of the condensible-gas density, even at the end of the condensation process. Numerical calculations[15] based on an approximate solution of the Boltzmann equation indicate that these small fractions of light incondensible gases will not reduce the condensation rate by more than 10%, so we ignore this effect in our calculations.

D. Condensation in a Porous Bed

The use of a carbon first layer over a BeO bed (used as a neutron multiplier) requires that little carbon vapor should penetrate to the BeO; otherwise, large amounts of incondensible CO gas will be produced.[16] Calculations[16] show that for a pumping speed of 10^5 L s^{-1}, about 0.01 g of carbon per shot can be allowed through the bed. An increase in pumping speed increases the amount of carbon vapor that can penetrate the first layer, and vice versa. A conservative allowance would be 1 mg per pulse, which indicates that only one atom in 10^6 can penetrate the blanket, assuming that 1 kg is vaporized initially. For a condensation coefficient β, the probability of an atom not condensing after n_c collisions is $(1 - \beta)^{n_c}$. For $\beta = 0.5$, this means that a particle must experience at least 20 collisions to have a probability less than 10^{-6}

of escaping the bed. The mean free path for a bed with a packing fraction $\eta = 0.5$ is given by

$$l = \frac{V_f}{\pi N_s (d/2)^2} = \frac{2(1-\eta)}{3\eta} d = \frac{2d}{3},$$

where $V_f = V(1-\eta)$ is the free volume, d is the diameter of the spheres, and N_s is the number of spheres in the volume V. Thus the depth of the bed must be greater than

$$h = n_c l/3^{1/2} \simeq 8d.$$

The factor $1/3^{1/2}$ enters because the distance traveled through the bed in the z direction is that fraction of the total distance traveled. This depth is within the current design of the Cascade first wall, which comprises 10 layers. In this case the fraction of molecules getting through is about 1 in 10^8, a negligible fraction. These results imply that only a small amount of the bed is in contact with the carbon gas. After two layers, the density of a stationary gas would be $\sim$0.03, of the density just outside the bed. Clearly this continuous modeling is not accurate over such short distances as two layers; in addition, the gas will be moving. But it is clear that only one or two layers will be in significant contact with the condensing gas.

A gas molecule that enters the porous bed is rapidly condensed or reflected back into the gas. The typical thermal velocity of the molecules is about 10^3 m s^{-1}, and the diameter of the spheres making up the porous bed is 10^{-3} m; thus the collision frequency of gas molecules with the bed is about 10^6 Hz (since $l = 2d/3$). We can therefore treat the bed as a partially absorbing wall, whose effective condensation coefficient β_{eff} is given by the probability that a gas molecule that enters the bed never returns to the surface. Possible condensing and noncondensing trajectories are shown in Fig. 6. Although β_{eff} can be calculated as a function of β by numerical simulation, we make simple estimates of β_{eff}, taking β to be the value for monatomic carbon vapor at 1600 K, i.e., $\beta = 0.5$.

A gas molecule entering the bed has a probability β of condensing on its first collision. Assuming that the scattering of the reflected molecules is isotropic (as it is, for example, for rigid spheres), then half the reflected molecules, or a fraction $(1-\beta)/2$ of the originally incident molecules, are reflected back into the gas and the same fraction continue into the bed. Of those that continue into the bed, a fraction β are condensed on their first subsequent collision, so that a fraction $\beta(1-\beta)/2$ of the originally incident molecules are condensed on the second collision, etc. If we assume that any molecule reflected upwards escapes into the gas, we obtain a lower bound on the condensation coefficient:

$$\beta_{eff} = \beta + \beta(1-\beta)/2 + \beta[(1-\beta)/2]^2 + \ldots = \frac{2\beta}{1+\beta}.$$

Thus for small condensation coefficients a porous bed has an effective condensation coefficient almost double that of a plane wall; for $\beta = 0.5$, $\beta_{eff} \approx 0.67$. Of course, molecules that undergo a few collisions begin to penetrate the bed, so that reflection upwards does not necessarily mean that they escape into the gas. This is a small effect, so that a reasonable estimate of the condensation coefficient of monatomic carbon vapor on a graphite bed is 0.7.

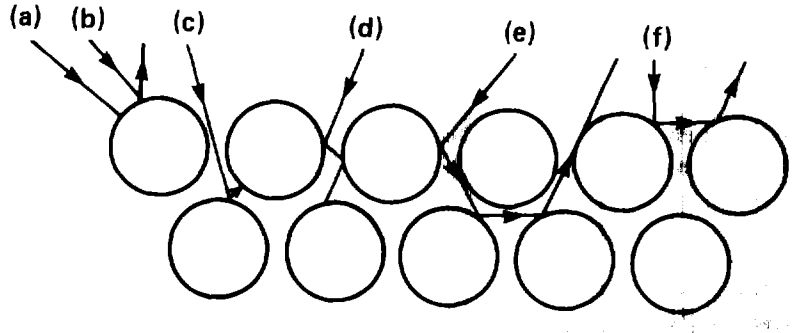

Figure 6. Condensation in a porous bed. Several possible condensation and reflection trajectories are shown: a. Condensation after one collision. b. Reflection into the gas after one collision. c, d. Condensation after multiple collisions. e, f. Reflection into the gas after multiple collisions.

E. Condensation Times for Carbon Vapor and Chamber Cooling

Using the effective condensation coefficient $\beta_{eff} = 0.7$ for a porous bed of carbon granules just found and the kinetic theory described in Sec. 2, we can estimate the condensation time t_c of the chamber for a carbon first wall. Assuming that the density must be decreased by a factor of 10^3, we have

$$t_c = \ln(1000)\tau = 6.9\tau ,$$

$$\tau = 0.085 \frac{m^{1/2}R}{\beta_{eff}T^{1/2}} \quad \text{ms} ,$$

where m is the dimensionless molecular weight (i.e., $m = 12$ for carbon), R is the chamber radius in meters, and T is the temperature in eV. For Cascade, with $R = 4$ m and $T = 0.2$ eV, we find $\tau = 3.8$ ms and $t_c = 26$ ms, well within the required time of 100 to 200 ms.

In our calculation of condensation [Eq. (1)] we considered only the mass flux leaving the system. However, the average energy of the condensing atoms is $2kT$, as against an average energy of $3/2kT$ in the bulk gas. This is because the more energetic particles condense more quickly, leaving behind a colder gas. The energy flux carried by the condensing particles is analogous to that given by Eq. (1) for the mass flux,

$$\int_0^\infty dv_1 \int_{-\infty}^{\infty} dv_2 \int_{-\infty}^{\infty} dv_3 \, nf(v)v_1 \left[\frac{1}{2}m\left(v_1^2 + v_2^2 + v_3^2\right)\right] = n\left(\frac{kT}{2\pi m}\right)^{1/2} 2kT .$$

The energy E_r of the reflected molecules can be described in terms of the thermal accommodation coefficient[13] α_t:

$$E_r = (1 - \alpha_t)(2kT) + \alpha_t(2kT_w) ,$$

where T_w is the wall temperature. Thus the net energy flux leaving the system is

$$n\left(\frac{kT}{2\pi m}\right)^{1/2} \left[2\beta_{eff}kT + 2(1 - \beta_{eff})\alpha_t k(T - T_w)\right] .$$

Let us first examine the case in which there is no thermal accommodation (i.e., $\alpha_t = 0$) and the noncondensing molecules are elastically reflected. This leads to two coupled equations for the density and temperature,

$$\dot{\rho} = -\frac{1}{\tau}(T/T_0)^{1/2}\rho ,$$

$$\dot{T} = -\frac{4}{3\tau}(T^3/T_0)^{1/2} ,$$

where

$$\tau^{-1} = 3\beta\left(\frac{kT_0}{2\pi mR^2}\right)^{1/2}$$

is the τ defined in Sec. 2. These equations can be solved to give

$$\rho(t) = \rho_0(1 + 2t/3\tau)^{-3/2} ,$$

$$T(t) = T_0(1 + 2t/3\tau)^{-2} . \qquad (5)$$

This is a much slower decay than was found when chamber cooling was ignored, and for the same final density, i.e., $10^{-3}\rho_0$, we find for carbon ($\tau = 3.8$ ms)

$$t_c = \frac{3}{2}(10^2 - 1)\tau = 560 \text{ ms} .$$

This condensation time is not acceptable from a practical point of view. However, the final temperature is predicted to be only 0.2 K: clearly, mechanisms for putting energy back into the chamber are important. It is worth noting that even at the final density ($10^{-3}\rho_0$) and temperature ($10^{-4}T_0$), the collision frequency is about 100 Hz, so the gas is still in a near-local equilibrium state.

If we have a degree of thermal accommodation α_t, then the minimum temperature in the chamber is given by

$$T_{min} = \frac{T_w}{\left[1 + \beta_{eff}/\alpha_t(1 - \beta_{eff})\right]} .$$

At this point the energy loss per molecule due to condensation is balanced by the energy gained from thermal accommodation with the surface. If the reflected carbon atoms are completely thermally accommodated (i.e., if $\alpha_t = 1$), and if $\beta_{eff} = 0.7$ as estimated earlier, the minimum temperature is $(1 - \beta_{eff})T_w$, i.e., about $0.3T_w$. It is interesting that a lower condensation coefficient may in fact *increase* the condensation rate by providing a

mechanism for putting energy back into the chamber. If cooling is included, so that decay is algebraic [as in Eq. (5)] until a minimum temperature of $0.3T_w$ is reached, and if constant-temperature exponential decay occurs thereafter, we find, for T_0 = 0.2 eV and T_w = 0.15 eV, and for the same initial conditions described earlier,

$t_c = 5.7 + 44.6 = 50$ ms .

These calculations indicate that although chamber cooling could significantly reduce the condensation rate (assuming that the gas temperature can be kept up to at least 10 to 50% of the wall temperature), the effect would not be fatal.

5. Future Experiments

In this report I have discussed effects that could reduce the condensation rate of vapors in the Cascade reactor from the acceptable value obtained by simple kinetic-theory calculations. I have shown that molecular first-wall materials are generally inappropriate because of the slow chemical recombination under the conditions found in Cascade. The estimates made here indicate that carbon is probably a suitable first-wall material, at least from the condensation standpoint. The calculations described here are considerable simplifications of a complex system, and it is therefore desirable to provide some experimental tests. A possible experiment is outlined below.

The spherical chamber (Fig. 7) has ports for the laser driver and diagnostics for measurement of temperature and pressure. In the center of the chamber is a relatively small spherical mirror. If a laser beam of exactly the same diameter as the mirror is focused on it, a nearly isotropic reflected will beam result. There is, of course, a small shadow region behind the mirror; the diagnostic equipment could be protected from the laser beam by placing it in this shadow. The inside of the chamber wall is coated with carbon; by varying the grain size of the powder, the effective surface for condensation can be adjusted to simulate the effect of a porous bed; the area should be about 1.5 times the flat-surface area. The chamber should be as large as possible, because chemical recombination times do not scale with the chamber radius, while hydrodynamic times do. On the other hand, the laser power available limits the chamber size. Typical Q-switched laser pulses are

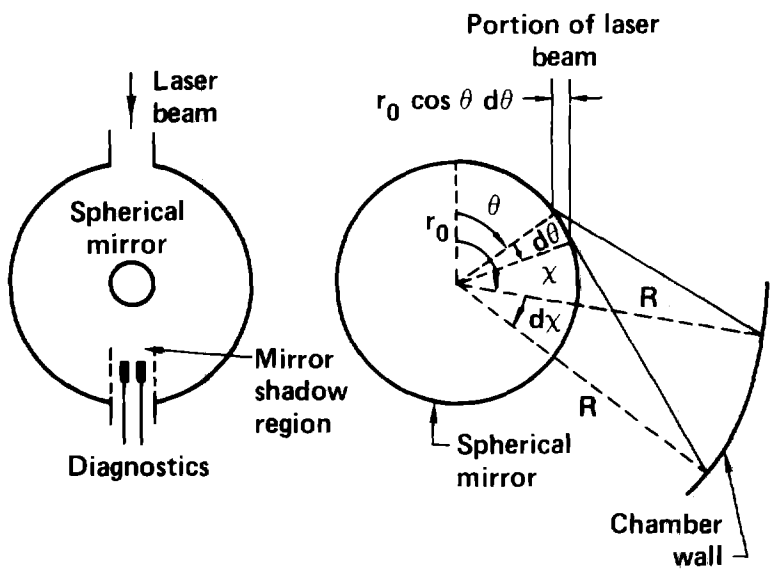

Figure 7. A possible experimental test of condensation. The spherical chamber contains a small spherical mirror illuminated by a single laser beam. The diagnostics to measure temperature and pressure can be placed in the shadow of the mirror to protect them from laser irradiation. Details of the reflected beam are shown in the second illustration. A small portion $r_0 \cos\theta\, d\theta$ of the beam is incident at a point on the mirror described by the polar angle θ. The reflected beam diverges and occupies a region $d\chi$ on the chamber wall described by the angle χ.

about 40 to 50 ns long. Internal energies of material vaporized by energy fluxes of up to 10^{12} W cm^{-2} have been reported.[17] Extrapolation of the data in Fig. 4.11 of Ref. 17 indicates that a peak energy flux of about 10^8 W cm^{-2} is required to produce carbon ions of an appropriate energy (10 eV per molecule, corresponding to 80 MJ kg^{-1}). The depth of material vaporized by a 40-ns pulse is probably about 10^{-6} m. The shorter pulse from the Novette laser (~1 to 5 ns) will vaporize less material and give it a higher energy. An appropriate total mass of vaporized material could be obtained by varying the chamber radius. In Cascade we have about 1 kg per 200 m^3, so if (for example) 1 μm of material is vaporized, an appropriate chamber radius is about 1 m (since the density of solid carbon is about 2×10^3 kg m^{-3}). A somewhat smaller chamber will probably be used, because less than 1 μm will probably be vaporized. Reduction in chamber radius by a factor of 10 from that of the real chamber will not critically affect the chemical processes. The estimates of dissociation rates obtained in Sec. 3(C) show that if the chamber radius is about 0.1 m or less, the gas may well converge on the center of the chamber before carbon dissociation is complete, thus hindering the subsequent recombination. Condensation times measured in such experiments may be unrealistically long when scaled to the dimensions of the Cascade chamber. The required laser power is about 10^{12} to $10^{13}R^2$ W, where R is in meters, so that chamber radii less than 0.5 m are within Novette's power range. It would therefore seem that experiments along these lines are plausible and should be investigated further.

6. Conclusions

The dissociation equilibria of three potential first-wall materials (BeO, SiC, and C) have been considered. Because of the low gas density, recombination essentially ceases after blowoff stops and condensation begins. Dissociation, on the other hand, is unhindered, and thus equilibrium estimates at the beginning of condensation are reasonable estimates of the degrees of dissociation during condensation.

The dissociation of the diatomic gases BeO and SiC was calculated from ideal-gas partition functions; for carbon, the theoretical ($1/p^2$) pressure dependence of the degree of dissociation was used to extrapolate the results of Leider et al.[8] to low pressure. Only the monatomic and triatomic forms of carbon, which are the dominant species at low pressure, were considered. At temperatures greater than 0.5 eV, all three materials were predicted to be completely dissociated at the beginning of condensation.

The high degree of dissociation of the diatomic gases, together with the high volatility of at least one of the constituent atoms (Be, O, or Si) makes them unsuitable as first-wall materials.

It is worth noting that ionization equilibrium is maintained down to very low pressures, because of the large collision cross section for ion recombination. The Saha equation indicates that the degree of ionization for carbon is about 0.001 at a temperature of 0.5 eV, so that we can assume that a neutral vapor is present.

The experimental condensation coefficient for monatomic carbon vapor condensing on a graphite surface at 1600 K is about 0.5. For the triatomic vapor, this coefficient is less than 0.1. The condensation of carbon therefore is assisted by the high degree of dissociation of the vapor.

The effective condensation coefficient might be reduced by the buildup of incondensible gas near the wall. Approximate solutions[15] of the Boltzmann equation, however, indicate that this will lead to less than a 10% reduction in the condensation rate. This is because of the low concentration (less than 10%) and the small mass of the incondensible-gas molecules.

The use of a carbon first wall over a BeO layer requires that little carbon vapor should penetrate to the BeO below, to avoid the production of large amounts of incondensible CO gas.[16] A conservative allowance is 1 mg of carbon per pulse, which means that the probability of penetration through the bed must be 10^{-6} or less, if the mass vaporized per pulse is 1 kg. For a condensation coefficient of 0.5, this probability corresponds to at least 20 collisions during passage through the bed. A kinetic-theory calculation of the mean free path of a molecule in the bed reveals that this requires about eight layers of carbon.

The rapid decrease in carbon-vapor density through the bed makes it somewhat difficult to calculate an effective condensation coefficient for the bed. However, since a molecule that enters the bed condenses very quickly (in less than 10^{-5} s), the bed can be treated as an absorbing wall, with an effective condensation coefficient given by the probability that a molecule that enters the bed

does not return to the bulk vapor. This problem is amenable to numerical simulation, but a simple estimate indicates that the condensation rate for a porous bed is about 50% greater than that for a planar wall. The estimated condensation times for carbon are 0.03 to 0.05 s, within the time constraints set by Cascade's 5- to 10-Hz repetition rate.

An experiment to check these condensation calculations has been proposed here.

Acknowledgments

Many people have contributed to my understanding of this problem: Lewis Glenn, William Hogan, Oscar Krikorian, Charles Orth, John Pitts, and David Young at LLNL; Robert Schmeider at Sandia National Laboratory, Livermore; Nathan Hoffman at Rockwell International Energy Technology Engineering Center, Canoga Park, Calif.; and Robert Peterson at the University of Wisconsin, Madison.

References

1. L. A. Glenn, *Nucl. Eng. Des.* **64**, 375 (1981); *Nucl. Eng. Des.* **69**, 75 (1982).
2. W. J. Hogan and C. D. Orth, Lawrence Livermore National Laboratory, Livermore, Calif., private communication (1985).
3. R. B. Peterson, University of Wisconsin, Madison, results from runs of the CONRAD computer code, private communication (1985).
4. D. A. McQuarrie, *Statistical Mechanics* (Harper and Row, New York, N.Y., 1976).
5. K. P. Huber and G. Herzberg, *Constants of Diatomic Molecules* (Van Nostrand, New York, N.Y., 1979).
6. G. Herzberg, *Spectra of Diatomic Molecules* (Van Nostrand, New York, N.Y., 1950).
7. G. A. Bird, *Molecular Gas Dynamics* (Clarendon Press, Oxford, 1976), pp. 5–6, 198–194.
8. H. R. Leider, O. H. Krikorian, and D. A. Young, *Carbon* **11**, 555 (1973).
9. M. Mitchner and C. H. Kruger, *Partially Ionized Gases* (Wiley-Interscience, New York, NY, 1973), pp. 457–469.
10. R. W. Zwanzig, *J. Chem. Phys.* **32**, 1173 (1960).
11. W. A. Chupka, J. Berkowitz, D. J. Meschi, and H. A. Tasman, *Adv. Mass. Spec.* **2**, 99 (1963).
12. R. J. Thorn and G. H. Winslow, *J. Chem. Phys.* **26**, 186 (1957).
13. J. P. Hirth and G. M. Pound, *Prog. Mater. Sci.* **11** (1963).
14. J. H. Pitts, *Int. J. Multiphase Flow* **6**, 329 (1980).
15. L. Pong and G. A. Moses, *Vapor Condensation in the Presence of A Non-Condensible Gas*, University of Wisconsin, Madison, Wis., UWFDM-565 (1984).
16. A. Darnell and N. J. Hoffman, *Non-Condensible Gas Phase Generation in the Cascade Reactor*, Rockwell International Energy Technology Engineering Center (ETEC), Canoga Park, Calif., unpublished report (1985).
17. J. F. Ready, *Effects of High Power Laser Radiation* (Academic Press, New York, N.Y., 1971).

PM/jr,js